Design of Self-Tuning SISO Partial-Form Model-Free Adaptive Controller for Vapor-Compression Refrigeration System

CHEN CHEN AND JIANGANG LU

State Key Laboratory of Industrial Control Technology, College of Control Science and Engineering, Zhejiang University, Hangzhou 310027, China

Corresponding author: Jiangang Lu (lujg@zju.edu.cn)

ABSTRACT Vapor-compression refrigeration systems (VCRS) are applied extensively in domestic, commercial and industrial refrigeration and are responsible for a high percentage of worldwide energy consumption. To achieve high energy efficiency, the application of advanced control methods in VCRS has increasingly attracted the attention of academia and industry. The model-free adaptive control (MFAC) strategy, as an important branch of advanced control research, encounters the problem of parameter tuning when applied to VCRS with strong nonlinearities. In this work, a parameter self-tuning methodology based on the self-learning and self-adapting properties of back propagation neural networks with the System Error set and/or Gradient Vector set as inputs is proposed to adjust the parameters utilized in SISO Partial-Form Model-Free Adaptive Control (SISO-PFMFAC). To test the performance of this novel methodology named SISO-PFMFAC-NNSEGV, qualitative and quantitative comparisons are carried out between the proposed method and the decentralized single PIDs given in the simulation platform provided by the benchmark PID 2018. The integral absolute error (*IAE*), the integral time-weighted absolute error (*ITAE*), the integral absolute variation of control signal (*IAVU*) and a combined index J_c are used to evaluate the performance. As a result, the proposed method shows the best performance with a higher tracking accuracy and less variation of the control signal with a combined index $J_c = 0.7088$, which represents a 29.1% improvement over the benchmark PID controller and a 9.6% improvement over the SISO-PFMFAC controller, making it a promising control method for vapor-compression refrigeration systems.

INDEX TERMS Partial-form model-free adaptive control, parameter self-tuning, back propagation neural networks, vapor-compression refrigeration system.

I. INTRODUCTION

Vapor-compression refrigeration systems (VCRS), which are widely used for domestic, commercial and industrial applications, are the leading technology worldwide in cooling generation, including air conditioning, refrigeration and freezing [1]. Heating, ventilating, and air conditioning (HVAC) processes account for approximately 30% of the total energy consumption worldwide, making the energy demand related to refrigeration systems an essential element of the overall energy mix [2], [3]. Therefore, considering the importance of the economy and the environment, it is necessary

The associate editor coordinating the review of this article and approving it for publication was Bo Shen.

to control refrigeration systems in a precise and efficient manner. Reference [4] focuses on the reduction of operating cost of HVAC systems, and reference [5] suggests that the evaporative-cooled condenser is one of the immediate solutions to the quest for efficient use of millions of residential air-conditioners around the world.

Refrigeration systems are closed cycles in which the refrigerant works in an inverse Rankine cycle through an evaporator, compressor, condenser and expansion valve. Though the expansion valve and the compressor, heat is transferred by the refrigerant from the evaporator secondary fluid to the condenser secondary fluid. To satisfy the expected cooling demand and maximize the energy efficiency, a controller is designed to track the references of the temperature of

the evaporator secondary fluid $T_{e,sec,out}$ and the refrigerant superheating degree T_{SH} at the evaporator outlet as efficiently as possible by manipulating the compressor speed N and the expansion valve opening Av in the presence of disturbances.

In recent years, many researchers have paid attention to the modeling and control of VCRS [6], [7]. Many model-based control (MBC) methods can be found in the literature, such as adaptive control [8], decoupling multivariable control [9], linear-quadratic-Gaussian (LQG) control [10], optimal control [11] and model predictive control [12]–[14]. These models can be developed based on the principles of thermodynamics [15], [16] or through system identification. However, due to the strong nonlinearities and strong coupling between variables of the VCRS, most researchers adopt model reduction or controller reduction, which introduces unmodeled dynamics while resulting in unsatisfactory control performance.

This motivates research on model-free control or data-driven control, which does not require any model information of the controlled system. Since the input and output measurement data of the system can precisely reflect valuable state information of the process operations and equipment, it becomes meaningful to design a controller by directly using the I/O data when an accurate model of the controlled plant is unavailable. PID [17] control, one of the traditional data-driven control methods, has been applied in the VCRS [18]. Meanwhile, some improved PID control methods such as nonlinear PID controller [19] and optimal controller identification based PID controller [20], also have an application in the VCRS. However, PID controller and its variants still remain the problems unsettled when controlling the VCRS with strong nonlinearities, which leads to unsatisfactory control performance.

Model-free adaptive control (MFAC) [21], an important branch of advanced control research, using only online I/O measurement data for controller design, has been applied to many systems, such as variable polarity plasma arc welding (VPPAW) [22], post-combustion carbon capture (PCC) processes [23], multi-agent systems consensus tracking [24], AC/DC microgrids [25], *etc.*, which demonstrates its ability to control complex systems. The single input and single output (SISO) MFAC based on the partial-form dynamic linearization technique (SISO-PFMFAC) is a promising approach to control a class of SISO nonlinear discrete-time systems and has better adaptability to complex systems. However, to achieve accurate and effective control, choosing appropriate and robust controller parameters is also of great importance for an actual system. In the literature, there are few methods outlined for the parameter tuning of MFAC. Reference [26] uses a virtual reference feedback tuning (VRFT) approach, which is an offline parameter tuning method that requires a large number of I/O data pairs of the controlled plant in an opened or closed loop. dos Santos Coelho and Coelho [27] optimize MFAC using a chaotic particle swarm approach, which needs a large number of iterations and is not suitable in practice.

In this paper, a novel online parameter self-tuning approach of SISO-PFMFAC based on a back propagation neural network with a system error set and a gradient vector set as inputs (SISO-PFMFAC-NNSEGV) is proposed for the control of a vapor-compression refrigeration system provided by the benchmark PID 2018 [18]. The proposed controller achieves better tracking performance and less variation of the control signal than the fixed parameter controller SISO-PFMFAC and the benchmark PID controller. Therefore, it can be concluded that the self-tuning SISO partial-form model-free adaptive controller has excellent practical application prospects in the control of vapor-compression refrigeration systems.

The main contributions of this paper are as follows. 1) The proposed method is a pure data-driven approach, which is merely based on the I/O data without using any model information of the vapor-compression refrigeration system, thus any unmodeled dynamic problems existed in the model-based control methods are avoided. 2) To achieve high energy efficiency while satisfying the cooling demand, the important parameters in the SISO-PFMFAC controller can be self-tuned online based on the BP neural network, which is also depends directly on the measured I/O data rather than any model information of the vapor-compression refrigeration system. 3) The proposed method presents the best performance with higher tracking accuracy on the temperature of the evaporator secondary fluid and the refrigerant superheating degree, while requires less variation of the control signals for the expansion valve opening and the compressor speed.

The rest of this paper is organized as follows. Section II reviews the benchmark VCRS and then provides the control objective. Section III contains the problem formulation including dynamic linearization for VCRS and controller design for SISO partial-form model-free adaptive control based on a neural network. The results and discussion are provided in section IV, and section V concludes this paper.

II. BENCHMARK OVERVIEW

The benchmark PID 2018 [18] provides a platform for researchers to test their recent developments in the design of controllers for VCRS. Full documentation on the system and MATLAB files can be obtained from http://www.dia.uned.es/~ fmorilla/benchmarkPID2018/.

The schematic of the refrigeration cycle is shown in Fig.1, where the main components are the evaporator, condenser, variable speed compressor, and expansion valve. The objective of the cycle is to remove heat from the secondary flux at the evaporator and reject heat at the condenser by transferring it to the secondary flux. The refrigerant circulates through the four main components and goes through four processes in sequence: (a) The refrigerant enters the evaporator at low temperature and pressure and it evaporates while removing heat from the evaporator secondary flux; (b) The evaporated refrigerant is taken into the compressor, with the pressure and temperature increasing, and then enters the condenser; (c) The refrigerant condenses and may become a subcooled liquid while transferring heat to the condenser secondary
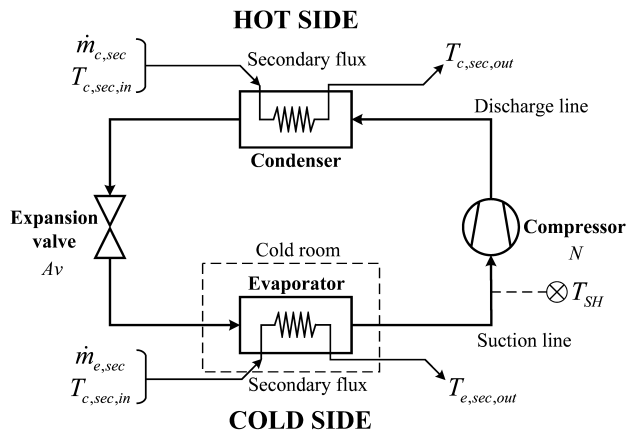
FIGURE 1. Schematic picture of the vapor-compression refrigeration cycle.

flux; (d) Controlled by the expansion valve, the refrigerant at low pressure and temperature enters the evaporator for the next cycle.

The main control objective of the refrigeration system is to meet the cooling demand, which can be expressed as a reference on the outlet temperature of the evaporator secondary flux $T_{e,sec,out}$ with the disturbance of the mass flux $\dot{m}_{e,sec}$ and the inlet temperature $T_{e,sec,in}$. With respect to the condenser, the inlet temperature $T_{e,sec,in}$ and the secondary mass flux $\dot{m}_{c,sec}$ are also considered disturbances. Furthermore, the generation of the cooling power is also intended to be as efficient as possible, which can be achieved by controlling the degree of super heating T_{SH}. Therefore, the controller is designed to get $T_{e,sec,out}$ and T_{SH} to track their references as efficiently as possible by manipulating the compressor speed N and the expansion valve opening Av in the presence of disturbances that are included in Table 1.

TABLE 1. Disturbance variables.

Variables	Description	Units
$T_{c,sec,in}$	Inlet temperature of the condenser secondary flux	$°C$
$\dot{m}_{c,sec}$	Mass flow of the condenser secondary flux	g s^{-1}
$P_{c,sec,in}$	Inlet pressure of the condenser secondary flux	bar
$T_{e,sec,out}$	Inlet temperature of the evaporator secondary flux	$°C$
$\dot{m}_{e,sec}$	Mass flow of the evaporator secondary flux	g s^{-1}
$P_{e,sec,in}$	Inlet pressure of the evaporator secondary flux	bar
T_{surr}	Compressor surroundings temperature	$°C$

The structure of the decentralized single PID controller included by default in the benchmark is shown in Fig. 2, where $T_{e,sec,out}$ and T_{SH} are controlled by means of the expansion valve Av and the compression speed N, respectively, and the transfer functions used within the default controller are described in Table 2 with a sampling time of 1 second. Note that the disturbance information is not used;

TABLE 2. Discrete transfer functions used within the default controller.

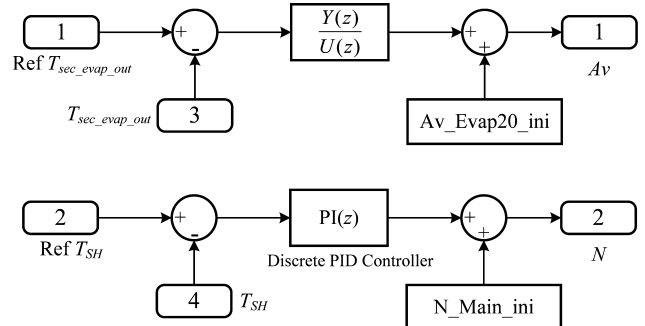| Controller	Transfer function
$T_{e,sec,out} - Av$	$\dfrac{-1.0136 - 0.0626z^{-1} + 0.9988z^{-2}}{1 - 1.9853z^{-1} + 0.9853z^{-2}}$
$T_{SH} - N$	$\dfrac{0.42 - 0.02z^{-2}}{1 - z^{-1}}$

FIGURE 2. The structure of the decentralized single PID controller included by default in the benchmark.

thus, the two SISO controllers operate without feed forward compensation.

III. PROBLEM FORMULATION

A. DYNAMIC LINEARIZATION TECHNIQUE FOR REFRIGERATION SYSTEM

Due to the strong nonlinearities and strong coupling between variables of the vapor-compression refrigeration system, most of the research on model-based control methods adopt model reduction or controller reduction, which introduces unmodeled dynamics while resulting in unsatisfactory control performance.

However, thanks to the development of electronic techniques, it has become possible to extract all valuable state information from a large amount of I/O data. Taking advantage of the I/O data, a virtual equivalent dynamic linearization data model is established along the dynamic operation points of the closed loop system by using a dynamic linearization technique [21], instead of identifying a nonlinear model of the vapor-compression refrigeration system, thereby avoiding the unmodeled dynamics and facilitating the controller design.

Consider the following discrete-time SISO nonlinear refrigeration process:

$$y_s(k+1)$$
$$= f_s(y_s(k), \cdots, y_s(k - n_{y_s}), u_s(k), \cdots, u_s(k - n_{u_s})) \quad (1)$$

where $s = 1, 2$; $y_1(k)$, $y_2(k) \in \mathbf{R}$ are the system outputs $T_{e,sec,out}(k)$ and $T_{SH}(k)$, respectively; $u_1(k)$, $u_2(k) \in \mathbf{R}$ are the control inputs $Av(k)$ and $N(k)$, respectively; n_{y_1}, n_{y_2} are the unknown orders of $y_1(k)$ and $y_2(k)$, respectively; n_{u_1}, n_{u_2} are unknown orders of $u_1(k)$ and $u_2(k)$, respectively; $f_1(\cdots)$: $\mathbf{R}^{n_{u_1}+n_{y_1}+2} \mapsto \mathbf{R}, f_2(\cdots)$: $\mathbf{R}^{n_{u_2}+n_{y_2}+2} \mapsto \mathbf{R}$ are unknown nonlinear functions; $\mathbf{R}$ is the set of all real numbers.

Define $\mathbf{U}_{L_s}(k) \in \mathbf{R}^{L_s}$ as the following vector that contains all control input in a sliding time window of $[k - L_s + 1, k]$.

$$\mathbf{U}_{L_s}(k) = [u_s(k), \cdots, u_s(k - L_s + 1)]^{\mathrm{T}} \quad (2)$$

where the two positive integers L_1, $L_2 > 1$ are linearization length constants (LLC) for the control inputs of Av and N, respectively.

The following assumptions for nonlinear dynamics are given to facilitate our analysis.

Assumption 1: The partial derivative of the nonlinear function $f_s(\cdots)$ with respect to $u_s(k)$ is continuous.

Assumption 2: The system (1) is a generalized Lipschitz function; that is, if $\Delta \mathbf{U}_{L_s} \neq 0$, $|\Delta y_s(k+1)| \leq b |\Delta \mathbf{U}_{L_s}(k)|$ holds for any k, where $\Delta y_s(k+1) = y_s(k+1) - y_s(k)$, $\Delta \mathbf{U}_{L_s}(k) = \mathbf{U}_{L_s}(k) - \mathbf{U}_{L_s}(k-1)$ and b is a positive constant.

Remark 1: These assumptions imposed on the refrigeration system are reasonable and acceptable from a practical viewpoint. *Assumption 1* is a general condition for controller design. *Assumption 2* indicates that the change rate of the refrigeration system output $T_{e,sec,out}$, T_{SH} corresponding to the change rate of the control input Av, N is bound. From an energy point of view, if the change in the control input energy is finite, the rate of change in the output energy cannot tend to infinity.

Theorem 1: For the refrigeration system (1) satisfying *Assumption 1* and *Assumption 2*, there must exist a $\phi_{s,L_s}(k)$, called pseudo gradient (PG), such that if $\|\Delta \mathbf{U}_{L_s}(k)\| \neq 0$, the system (1) can be described as the following partial form dynamic linearization (PFDL) model:

$$\Delta y_s(k+1) = \phi_{s,L_s}^{\mathrm{T}} \Delta \mathbf{U}_{L_s}(k) \quad (3)$$

where $\phi_{s,L_s} = [\phi_{s,1}, \cdots, \phi_{s,L_s}]^{\mathrm{T}} \in \mathbf{R}^{L_s}$ and it satisfies $|\phi_{s,L_s}| \leq c$, where c is a positive constant.

B. SISO-PFMFAC CONTROLLER DESIGN

In a vapor-compressor refrigeration system, rapid changes in the control inputs Av and N would harm the system while decreasing the energy efficiency. Therefore, the weighted one-step-ahead control input criterion function is considered:

$$J(u_s(k)) = |y_s^*(k+1) - y_s(k+1)|^2 + \lambda_s |u_s(k) - u_s(k-1)|^2 \quad (4)$$

where $\lambda_1, \lambda_2 > 0$ are weighting factors that are introduced to constrain the control inputs of Av and N from changing too quickly, respectively, and $y_1^*(k)$, $y_2^*(k)$ are the expected outputs values of $T_{e,sec,out}$, T_{SH}, respectively.

By setting the derivative of (4) with respect to $u_s(k)$ equal to zero, an iterative function is obtained:

$$u_s(k) = u_s(k-1) + \frac{\rho_{s,1}\phi_{s,1}(k)(y_s^*(k+1) - y_s(k))}{\lambda_s + |\phi_{s,1}(k)|^2}$$

$$- \frac{\phi_{s,1}(k) \sum_{p=2}^{L_s} \rho_{s,p}\phi_{s,p}(k)\Delta u_s(k-p+1)}{\lambda_s + |\phi_{s,1}(k)|^2} \quad (5)$$

where $\rho_{s,p} \in (0,1]$, $(p = 1, 2, \cdots, L_s)$ is introduced as a penalty factor for a more general and flexible controlling rule. In addition, we noticed that λ_s is not only a penalty factor on $\Delta u_s(k)$ but also a part of the denominator in (5); thus $\rho_{s,p}$ and λ_s are important parameters for the SISO-PFMFAC scheme.

Obviously, it is difficult to derive a specific expression for the solution of the time-varying parameter ϕ_{s,L_s}, so a certain approximation algorithm is essential for the description of the refrigeration system. Similar to (4), a weighted one-step-ahead cost function of PG is considered:

$$J(\phi_{s,L_s}(k)) = \left| y_s(k) - y_s(k-1) - \phi_{s,L_s}^{\mathrm{T}}(k)\Delta \mathbf{U}_{L_s}(k-1) \right|^2$$

$$+ \mu_s \left\| \phi_{s,L_s}(k) - \hat{\phi}_{s,L_s}(k-1) \right\|^2 \quad (6)$$

By setting the derivative of (6) with respect to ϕ_{s,L_s} equal to zero, an iterative function is obtained:

$$\hat{\phi}_{s,L_s}(k) = \hat{\phi}_{s,L_s}(k-1)$$

$$+ \frac{\eta_s \Delta \mathbf{U}_{L_s}(k-1)(y_s(k) - y_s(k-1) - \hat{\phi}_{s,L_s}^{\mathrm{T}}(k-1)\Delta \mathbf{U}_{L_s}(k-1))}{\mu_s + \left\| \Delta \mathbf{U}_{L_s}(k-1) \right\|^2} \quad (7)$$

where $\eta_s \in (0, 2]$ is introduced as a step size constant for a more general and flexible approximation algorithm. $\hat{\phi}_{s,L_s}(k)$ is the approximation of ϕ_{s,L_s}, and μ_s is a weighting factor that is introduced to punish sudden changes in ϕ_{s,L_s}.

Moreover, to ensure that the adaptive law has strong tracking capability on time-varying parameters, a reset algorithm is considered in the following structure:

$$\hat{\phi}_{s,L_s}(k) = \hat{\phi}_{s,L_s}(1),$$

$$\text{if } \left\| \hat{\phi}_{s,L_s}(k) \right\| \leq \varepsilon \text{ or } \left\| \Delta \mathbf{U}_{L_s}(k-1) \right\|$$

$$\leq \varepsilon \text{ or } sign(\hat{\phi}_{s,1}(k)) \neq sign(\hat{\phi}_{s,1}(1)) \quad (8)$$

where ε is a sufficiently small positive constant and $\hat{\phi}_{s,L_s}(1)$ is the initial estimation value of $\hat{\phi}_{s,L_s}(k)$.

C. THE PROPOSED SISO-PFMFAC-NNSEGV CONTROL METHODOLOGY

The vapor-compression refrigeration system is complex, and its dynamics are difficult to identify and subject to environmental uncertainties. Therefore, a fixed-parameter SISO-PFMFAC may not be well adapted to the changes in operating conditions, since the refrigeration process is non-linear, time-variant and coupled. However, the fine tuning of SISO-PFMFAC is still a laborious, time-consuming and cost-consuming task that requires experts with knowledge in both control theory and process information. Although there are already some methods for offline parameter tuning in the literature as mentioned in section I, it is difficult to apply these methods to an actual system due to their limitations. Therefore, online self-tuning method SISO-PFMFAC-NNSEGV based on a BP neural network, a more accurate and more efficient control methodology, is proposed for VCRS with the advantage of simplicity, robustness and ease of implementation.

1) BPNN OVERVIEW

In the literature, there have been many reports on the application of BPNN and its variants in control systems, such as soft soil [28], inverters [29], hot-rolling steel [30], *etc.*, which demonstrates the self-learning and self-adapting capabilities of BPNN. As one of the feedforward networks, BPNN is commonly used by the gradient descent optimization algorithm to adjust the weight of neurons by calculating the gradient of the loss function. In general, the inputs of BPNN for parameter adjustment always rely on the system error $e_s(k) = y_s^*(k) - y_s(k)$ or the combination of $e_s(k)$, $\sum\limits_{t=0}^{k} e_s(t)$ and $e_s(k) - e_s(k-1)$, which contain all the information of the output. However, the dynamics of the control inputs should also be taken into consideration for BPNN because they reflect the sensitivity of the system to varying parameters, which are important information for the control of an actual system. In this paper, the BPNN with the system error set and gradient vector set of control input as learning signals is applied to obtain a more accurate trajectory and achieve high energy efficiency by auto-adjusting the parameters used in SISO-PFMFAC, with a simulation on the benchmark PID 2018.

2) LEARNING ALGORITHM FOR BPNN

It is known that, without limiting the number of hidden nodes, a BP neural network with three layers can achieve any nonlinear mapping. In this work, a BPNN with the system error set and gradient vector set as inputs is shown in Fig.3.
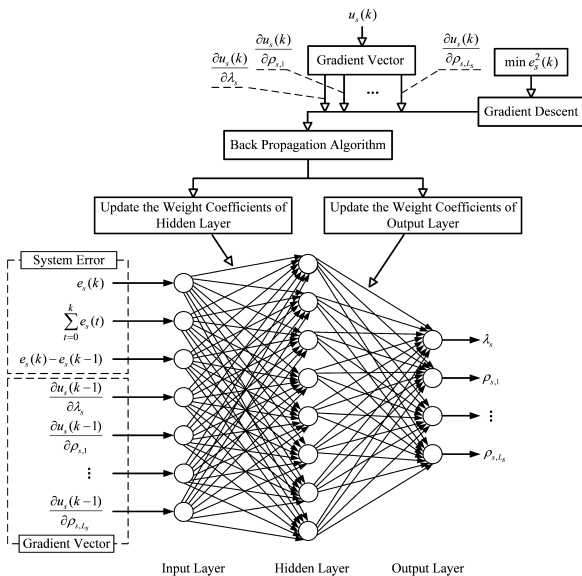

FIGURE 3. Structure of BPNN for self-tuning of parameters in SISO-PFMFAC.

The input layer has $L_s + 4$ nodes, corresponding to three combined system errors and $L_s + 1$ gradient vectors. The output layer has $L_s + 1$ nodes, corresponding to λ_s and $\rho_{s,p}$ used in SISO-PFMFAC. The nodes of the hidden layer are

calculated by the following formula:

$$h = \sqrt{m + n} + \alpha \tag{9}$$

where h, m and n denote the nodes of the hidden, input and output layers, respectively and α is a constant between 0 and 10.

- The input variables are $x_{sj}(j = 1, \cdots, L_s + 4)$

$$x_{sj} = \left[e_s(k), \sum_{t=0}^{k} e_s(t), e_s(k) - e_s(k-1), \frac{\partial u_s}{\lambda_s}, \frac{\partial u_s}{\rho_{s,1}}, \cdots, \frac{\partial u_s}{\rho_{s,L_s}} \right] \tag{10}$$

- The input and output of the hidden layer

$$hnet_{si}(k) = \sum_{j=1}^{L_s+4} \omega_{sij} x_{sj}(k) \tag{11}$$

$$hide_{si}(k) = f(hnet_{si}(k)), \quad i = 1, 2, \ldots, M_s \tag{12}$$

where ω_{sij} are the connection weight parameters between the input layer and hidden layer and M_s is the hidden neurons. The activation function of the hidden layer is as follows:

$$f(x) = \frac{e^x - e^{-x}}{e^x + e^{-x}} \tag{13}$$

- The input and output of the output layer are

$$onet_{sl}(k) = \sum_{i=1}^{M_s} \omega_{sli} hide_{si}(k)$$

$$out_{sl}(k) = g(onet_{sl}(k)) \quad l = 1, \cdots, L_s + 1$$

$$\lambda_s = out_{s1}(k)$$

$$\rho_{s,p} = out_{s(p+1)}(k) \quad p = 1, \cdots, L_s \tag{14}$$

where ω_{sli} are the connection weight parameters between the hidden layer and output layer. The activation function of the output layer is as follows:

$$g(x) = \frac{e^x}{e^x + e^{-x}} \tag{15}$$

- The dynamic learning performance index J_s for single SISO-PFMFACs is described as follows:

$$J_s = \frac{1}{2}[y_s^*(k+1) - y_s(k+1)]^2 = \frac{1}{2} e_s^2(k+1) \tag{16}$$

The partial derivative of J_s with respect to the weighting coefficients ω_{sli} and ω_{sij} can be obtained by applying the chain rule:

$$\Delta\omega_{sli}(k+1) = -\beta_s \frac{\partial J_s}{\partial \omega_{sli}} + \alpha_s \Delta\omega_{sli}(k)$$

$$\frac{\partial J_s}{\partial \omega_{sli}} = \frac{\partial J_s}{\partial y_s(k+1)} \frac{\partial y_s(k+1)}{\partial u_s(k)} \frac{\partial u_s(k)}{\partial out_{sl}(k)} \frac{\partial out_{sl}(k)}{\partial onet_{sl}(k)}$$
$$\times \frac{\partial onet_{sl}(k)}{\partial \omega_{sli}}$$

$$\Delta\omega_{sij}(k+1) = -\beta_s \frac{\partial J_s}{\partial \omega_{sij}} + \alpha_s \Delta\omega_{sij}(k)$$
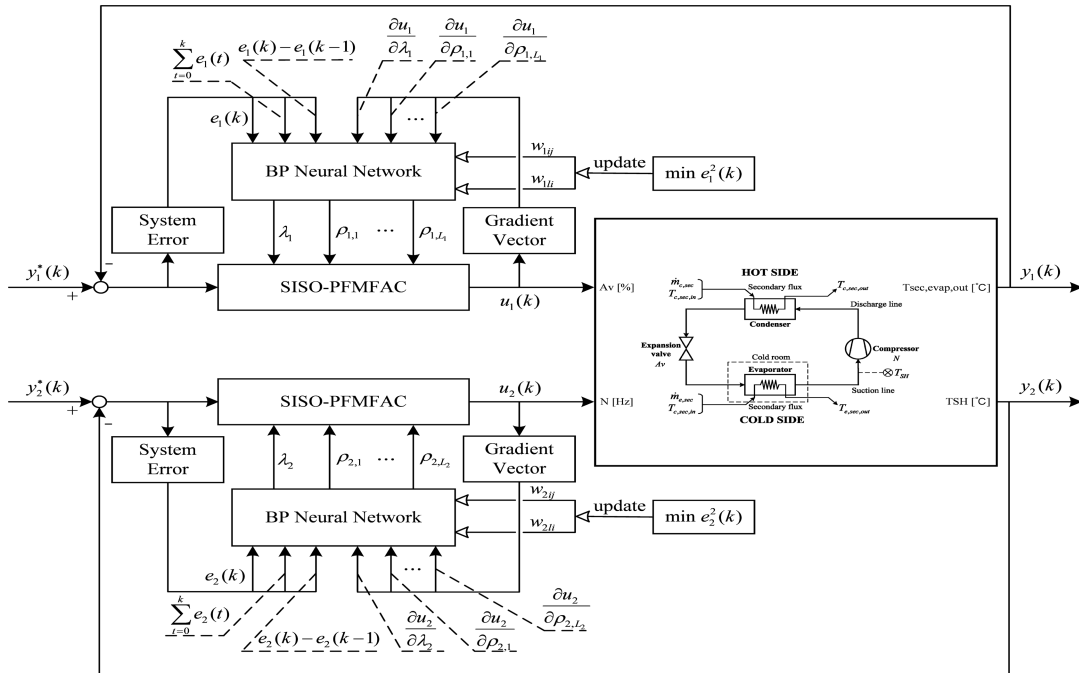
FIGURE 4. Block diagram of a refrigeration benchmark process controlled by the SISO-PFMFAC-NNSEGV scheme.

$$\frac{\partial J_s}{\partial \omega_{sij}} = \frac{\partial J_s}{\partial y_s(k+1)} \frac{\partial y_s(k+1)}{\partial u_s(k)} \frac{\partial u_s(k)}{\partial out_{sl}(k)} \frac{\partial out_{sl}(k)}{\partial onet_{sl}(k)}$$
$$\times \frac{\partial onet_{sl}(k)}{\partial hide_{si}(k)} \frac{\partial hide_{si}(k)}{\partial \omega_{sij}} \tag{17}$$

where α_s and β_s are the inertia coefficient and learning rate, respectively. The partial derivatives of u_s with respect to λ_s and $\rho_{s,p}$ are as follows:

$$\frac{\partial u_s(k)}{\partial \lambda_s} = -\frac{\rho_{s,1}\phi_{s,1}(k)(y_s^*(k+1) - y_s(k))}{(\lambda_s + |\phi_{s,1}(k)|^2)^2}$$
$$-\frac{\phi_{s,1}(k)\sum_{p=2}^{L_s} \rho_{s,p}\phi_{s,p}(k)\Delta u_s(k-p+1)}{(\lambda_s + |\phi_{s,1}(k)|^2)^2} \tag{18}$$

$$\frac{\partial u_s(k)}{\partial \rho_{s,1}} = \frac{\phi_{s,1}(k)(y_s^*(k+1) - y_s(k))}{\lambda_s + |\phi_{s,1}(k)|^2} \tag{19}$$

$$\frac{\partial u_s(k)}{\partial \rho_{s,p}} = -\frac{\phi_{s,1}(k)\phi_{s,p}(k)\Delta u_s(k-p+1)}{\lambda_s + |\phi_{s,1}(k)|^2} \quad 2 \le p \le L_s \tag{20}$$

- The adjustment of the weight coefficients ω_{sli} and ω_{sij} is expressed as

$$\Delta w_{sli}(k+1) = \beta_s o\delta_{sl} hide_{si}(k) + \alpha_s \Delta w_{sli}(k)$$
$$o\delta_{sl} = e_s(k+1)sign\left(\frac{\partial y_s(k+1)}{\partial u_s(k)}\right)$$
$$\times \frac{\partial u_s(k)}{\partial out_{sl}} g'(onet_{sl}(k))$$
$$\Delta w_{sij}(k+1) = \beta_s h\delta_{si} x_{sj}(k) + \alpha_s \Delta w_{sij}(k)$$

$$h\delta_{si} = f'(hnet_{si}(k))\sum_{l=1}^{L_s+1} o\delta_{sl}w_{sli}(k) \tag{21}$$

3) STRUCTURE OF THE PROPOSED CONTROLLER FOR A REFRIGERATION SYSTEM

The proposed controller based on BPNN, which is designed by combining the SISO-PFMFAC strategy with a neural network, has created a new concept and a new tool for the control of VCRS. The block diagram of the proposed controller called SISO-PFMFAC-NNSEGV used in the refrigeration benchmark process can be set up as depicted in Fig. 4. Both closed loops use the same control scheme of single SISO-PFMFACs, and the parameters used in the controllers can be self-tuned online separately. In addition, the initial conditions of the two control schemes can be chosen for a particular problem depending on the difference in the characteristics of the two closed loops.

4) FLOW CHART AND SOFTWARE

To briefly describe the proposed method, a relevant flow chart is presented in Fig. 5, showing the novel control scheme used in the refrigeration system step by step. The linearization length constants L_1 and L_2, varying from 1 to $n_{y_s} + n_{u_s}$, usually depend on the complexity of the system, and in this work, $L_1 = L_2 = 2$ are chosen for the refrigeration process. In addition, considering that the gradient vector set for the BPNN input is the previous information at time $k-1$, the derivatives of $Av(k)$, $N(k)$ with respect to $\rho_{s,p}$, λ_s are stored for the next time in each iteration, as indicated by the dashed line. All
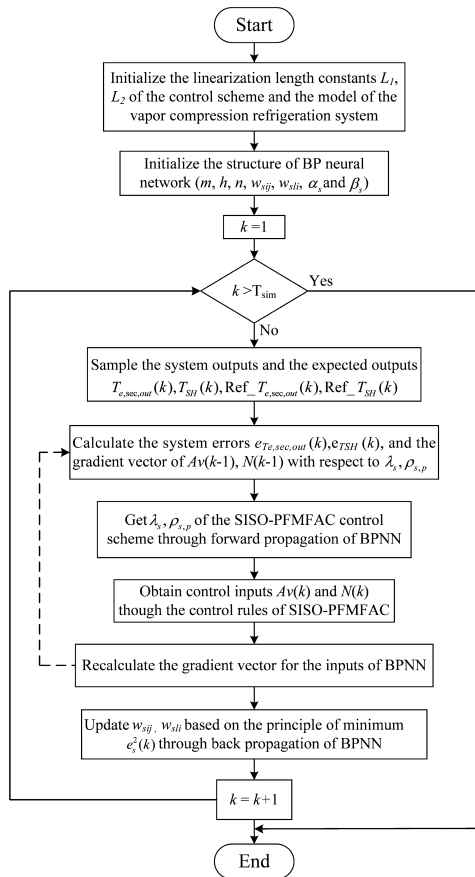
FIGURE 5. Flow chart describing the SISO-PFMFAC-NNSEGV control method.

the algorithms in this work were implemented in MATLAB 2017b (Mathworks Inc., USA).

IV. RESULTS AND DISCUSSION

In this section, the performance of SISO-PFMFAC-NNSEGV has been tested on vapor-compression refrigeration systems, keeping the default settings unchanged as described in sub-section 1). In subsection 2), the simulation results will be compared qualitatively and quantitatively with the given decentralized single PIDs. In addition, in order to validate that the BP neural network with the system error set and gradient vector set as learning signals has stronger robustness and adaptiveness, BPNNs with different inputs are also compared. As a result, the proposed model presents the best performance with higher tracking accuracy and less variation of the control signal, outperforming the benchmark controller.

A. INITIAL OPERATING CONDITIONS OF REFRIGERATION SYSTEM

The vapor-compression refrigeration system provided by the benchmark PID challenge is a two-input two-output system in the presence of seven disturbances, as described in section II. The initial operating points and the ranges of the manipulated variables, controlled variables and disturbances are described

TABLE 3. Initial operating points and input variable ranges.

Variables		Initial	Range	Units
Manipulated	Av	$\cong 48.79$	$[10-100]$	%
Variables	N	$\cong 36.45$	$[30-50]$	Hz
	$T_{c,sec,in}$	30	$[27-33]$	°C
	$\dot{m}_{c,sec}$	150	$[125-175]$	g s⁻¹
	$P_{c,sec,in}$	1	–	bar
Disturbances	$T_{e,sec,in}$	-20	$[-22--18]$	°C
	$\dot{m}_{e,sec}$	64.503	$[0.055-0.0075]$	g s⁻¹
	$P_{e,sec,in}$	1	–	bar
	T_{surr}	25	$[20-30]$	°C
Controlled	$T_{e,sec,out}$	$\cong -22.15$	–	°C
Variables	T_{SH}	$\cong 14.65$	–	°C

in Table 3. Particularly, it is worth mentioning that the manipulated variables Av and N are subjected to their limits, and are saturated within the system if the value is out of the range as indicated in Table 3, with consideration of the actual operating condition of the expansion valve and compressor speed. In addition, the influence of the inlet pressures of the secondary fluxes has not been studied, since their values affect only the calculation of the thermodynamic properties and it is expected that they will not change appreciably in a real application.

Furthermore, the desired references for the controlled variables and the major disturbances are the inlet temperature of the evaporator secondary flux $T_{e,sec,in}$ and the inlet temperature of the condenser secondary flux $T_{c,sec,in}$ which need to be compensated in the control objective, shown in Fig. 6 (a) and Fig. 6 (b), respectively.

B. COMPARISON RESULTS WITH DIFFERENT CONTROLLERS

In this subsection, qualitative and quantitative comparisons are carried out between the SISO-PFMFAC-NNSEGV controller and the default decentralized single PIDs provided by the benchmark PID 2018. In addition, to validate that the SISO-PFMFAC control scheme using a BP neural network with the system error set and gradient vector set as learning signals has stronger robustness and tracking ability, a set of comparisons are given in this subsection, including SISO-PFMFAC, an auto-tuned controller using BPNN only with the system error set as the learning signal, abbreviated as SISO-PFMFAC-NNSE, and an auto-tuned controller using BPNN only with the gradient vector set as the learning signal, abbreviated as SISO-PFMFAC-NNGV. The simulations always start from the initial operating points shown in Table 3, with a sampling time $T_s = 1$ s and simulation time $T_{sim} = 1200$ s.

To speed up the convergence of BPNN, pre-processing of data is considered first. Furthermore, the initial conditions of the SISO-PFMFAC-NNSEGV controller are: $L_1 = L_2 = 2$,
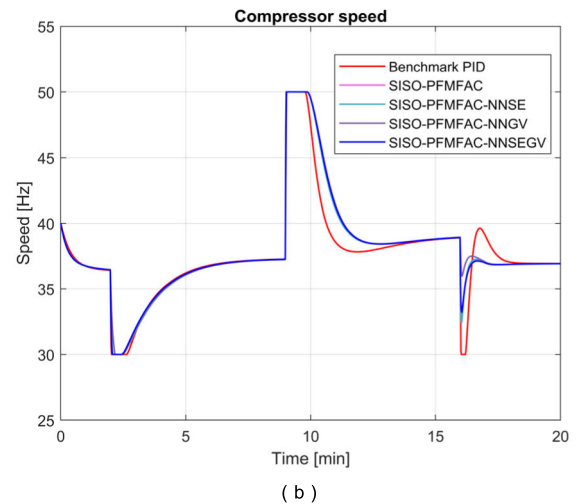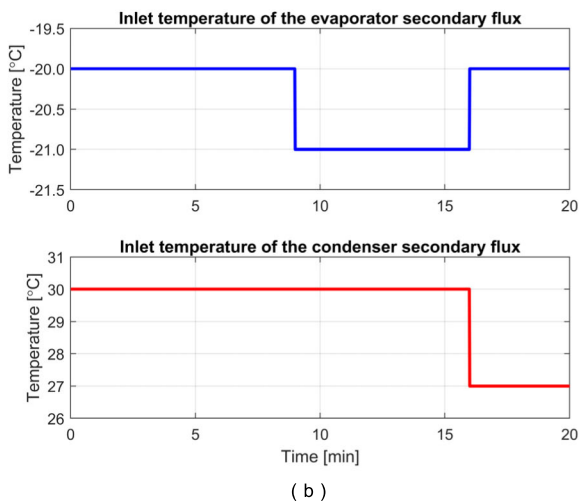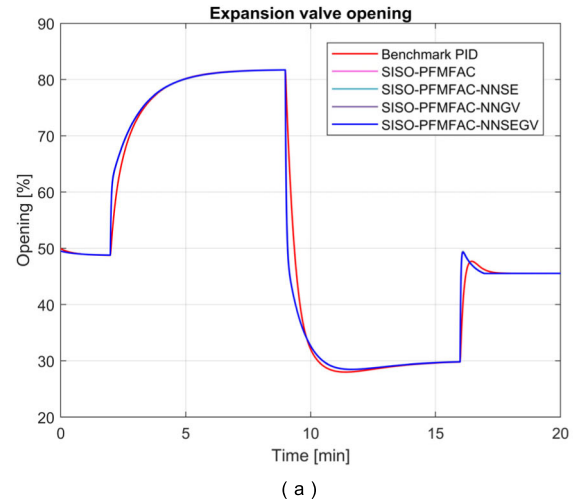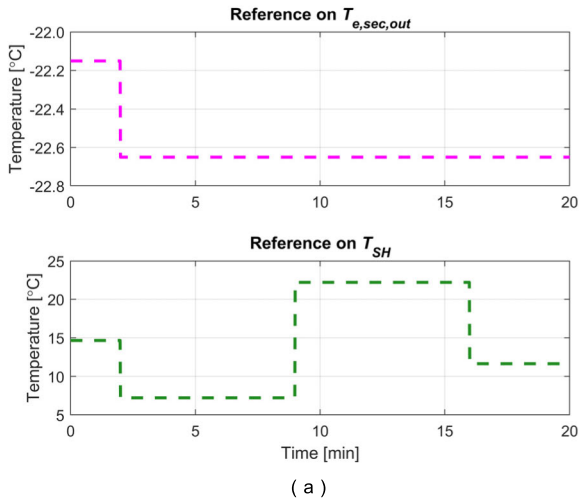
FIGURE 6. (a) The standard simulation generates changes in the reference on $T_{e,sec,out}$ and T_{SH}. (b) Two major disturbance variables $T_{e,sec,in}$ and $T_{c,sec,in}$.

FIGURE 7. Controlled inputs of (a) *Av* and (b) *N* for different controllers.

$\eta_1 = \eta_2 = 1$, $\mu_1 = \mu_2 = 1$, $\hat{\phi}_{1,L_1}(1) = \hat{\phi}_{2,L_2}(1) = [1, 0]^{\mathrm{T}}$, $\varepsilon = 10^{-5}$. The structure of both BPNNs is 6-8-3, the inertia coefficient $\alpha_1 = \alpha_2 = 0.1$, the learning rate $\beta_1 = \beta_2 = 0.3$, and the initial connection weights ω_{1ij}, ω_{1li}, ω_{2ij}, ω_{2li} are random between $[-0.5, \ 0.5]$.

Fig. 7 shows the manipulated variables *Av* and *N*, and that of the corresponding tracking performance of the controlled variables $T_{e,sec,out}$ and T_{SH} are given as shown in Fig. 8. It can be seen in Fig. 7(b), although the control response is saturated with respect to the compressor speed, it is important to observe that the proposed methods avoid saturation when applying the last disturbance of the inlet temperature of the evaporator secondary fluid $T_{e,sec,in}$ and the inlet temperature of the condenser secondary fluid $T_{c,sec,in}$ at $t = 16$ min, which requires less variation of the control signal while obtaining a tight control on T_{SH}. Moreover, as shown in Fig. 8 that the proposed controllers react quickly to sudden changes in references when disturbances are applied and show a significantly small overshoot compared with the

benchmark PID controller. Overall, the proposed controllers achieve better control performance than the decentralized single PIDs, with fast tracking performance and strong robustness.

Furthermore, to clearly compare the effects of different inputs for BPNN on the proposed self-tuning methods, the detailed tracking performance of $T_{e,sec,out}$ and T_{SH} are shown in Fig. 9-10, respectively. Fig. 9 (a) and (b) show the detailed tracking performance of $T_{e,sec,out}$ over the 2-2.1 min and 9-9.1 min intervals, and Fig. 10 (a) and (b) show the detailed tracking performance of T_{SH} over the 2-2.1 min and 9-9.1 min intervals.

As a result, the proposed controllers achieve better control performance especially than the default PID controller, with fast tracking performance and strong robustness. Besides, the parameter self-tuning approach proposed in this work using BP neural network with the system error set and gradient vector set as inputs performs better than that only with the system error set and that only with the gradient vector set as input. Thus, it can be concluded that the dynamic information
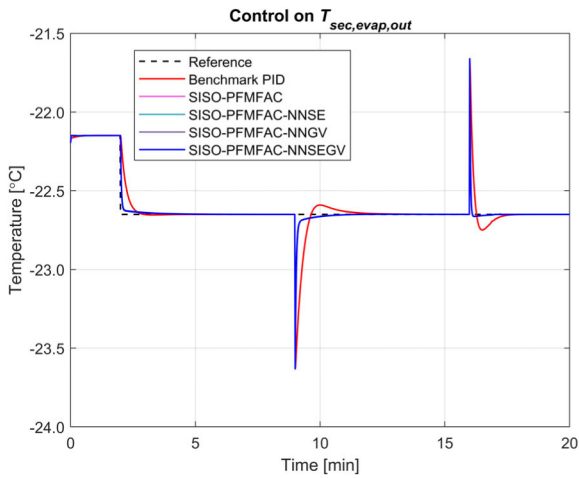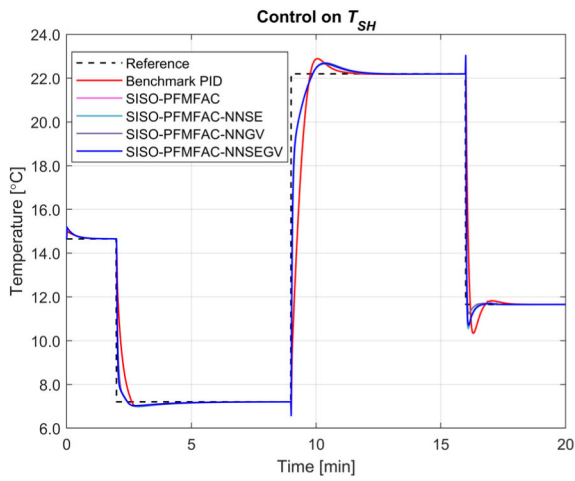
FIGURE 8. Tracking performance of (a) $T_{e,sec,out}$ and (b) T_{SH} for different controllers.

FIGURE 9. Detailed tracking performance of $T_{e,sec,out}$ over the 2-2.1 min (a) and 9-9.1 min (b) intervals for different controllers.

of the control input in BPNN is of great importance to the parameter tuning, which improves the adaptability of the controller by obtaining sufficient VCRS information.

The methodology proposed in this work increases the flexibility of λ_s and $\rho_{s,p}$ used in (5) and adapts well to the refrigeration system in the face of any disturbance. The self-tuning parameters of both SISO-PFMFAC-NNSEGV controllers are shown in Fig. 11-12, which are adjusted online according to the current system error. The parameters react quickly to sudden changes in the reference, showing a stronger self-adaptability than the fixed parameters used in SISO-PFMFAC.

To further analyse the performance of SISO-PFMFAC-NNSEGV, eight individual performance indices and one combined index J_c are used for quantitative comparison. The first two indices are the Ratio of Integral Absolute Error (RIAE), considering that the two controlled variables $T_{e,sec,out}$ and T_{SH} should track their references. The third index is the Ratio of Integral Time-weighted Absolute Error (RITAE) for $T_{e,sec,out}$, considering that the standard simulation includes
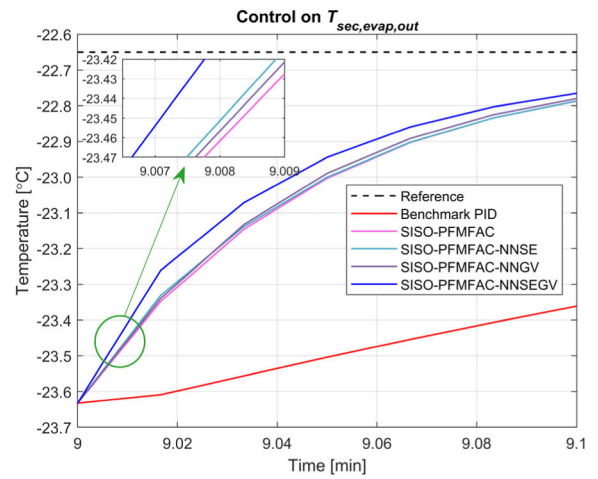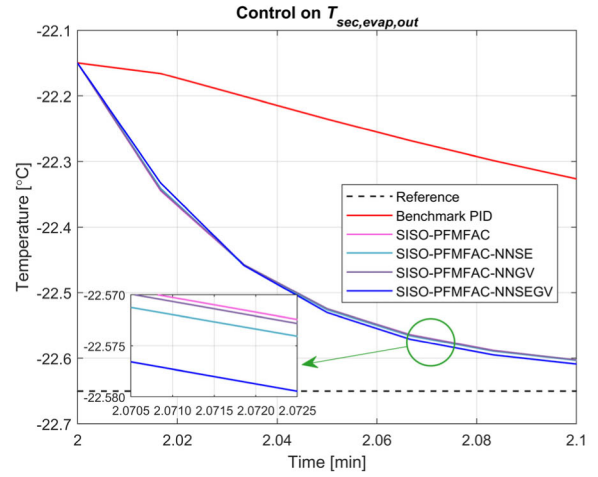
one sudden change in its reference. The fourth, fifth and sixth indices are the Ratios of Integral Time-weighted Absolute Error (RITAE) for T_{SH}, considering that the standard simulation includes three sudden changes in its reference. The seventh and eighth indices are the Ratios of Integral Absolute Variation of Control signal (RIAVU) for the two manipulated variables. The combined index J_c is a weighted average of the above seven indices. Note that t_c denotes the corresponding initial step time and t_s denotes the supposed worst-case settling time. All the indices mentioned above are described in (22)-(28).

$$IAE = \int_0^t |e_i(t)| \, dt \qquad (22)$$

$$ITAE = \int_{t_c}^{t_c+t_s} (t - t_c) |e_i(t)| \, dt \qquad (23)$$

$$IAVU_i = \int_0^t \left| \frac{du_i(t)}{dt} \right| \, dt \qquad (24)$$

$$RIAE_i(C_2, C_1) = \frac{IAE_i(C_2)}{IAE_i(C_1)} \qquad (25)$$

Control on T_{SH} (a)
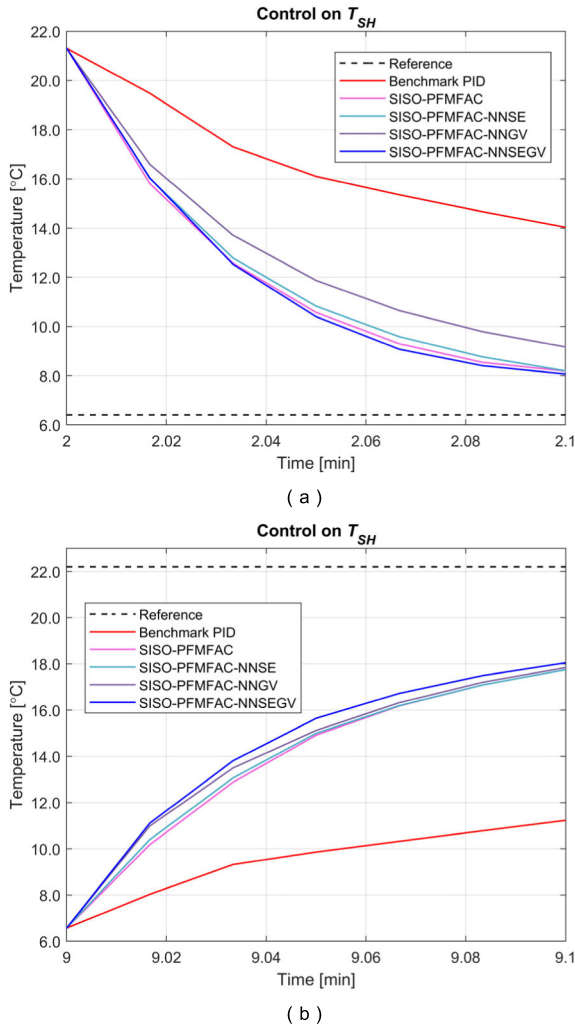

Control on T_{SH} (b)

FIGURE 10. Detailed tracking performance of T_{SH} over the 2-2.1 min (a) and 9-9.1 min (b) intervals for different controllers.

$$RITAE_i(C_2, C_1, t_c, t_s) = \frac{ITAE_i(C_2, t_c, t_s)}{ITAE_i(C_1, t_c, t_s)} \qquad (26)$$

$$RIAVU_i(C_2, C_1) = \frac{IAVU_i(C_2)}{IAVU_i(C_1)} \qquad (27)$$

$$J(C_2, C_1)$$
$$= \frac{\begin{aligned} &w_1 RIAE_1(C_2, C_1) + w_2 RIAE_2(C_2, C_1) \\ &+w_3 RITAE_1(C_2, C_1, t_{c1}, t_{s1}) + w_4 RITAE_2(C_2, C_1, t_{c2}, t_{s2}) \\ &+w_5 RITAE_2(C_2, C_1, t_{c3}, t_{s3}) + w_6 RITAE_2(C_2, C_1, t_{c4}, t_{s4}) \\ &+w_7 RIAVU_1(C_2, C_1) + w_8 RIAVU_2(C_2, C_1) \end{aligned}}{\sum_1^8 w_i}$$
$$(28)$$

Table 4 provides quantitative comparison indices that show the overall performance of the controllers. Analysing Table 4, it can be seen that all three self-tuning schemes have better tracking performance than the fixed-parameter controller SISO-PFMFAC, reflected in almost all relative indices and the combined index J_c, which demonstrate that the parameter self-tuning of SISO-PFMFAC is necessary

TABLE 4. Comparison of relative indices and combined index for different controllers.

Index	C_2 vs C_1	C_3 vs C_1	C_4 vs C_1	C_5 vs C_1
$RIAE_1(C_i,C_1)$	0.3024	0.3020	0.2994	0.2947
$RIAE_2(C_i,C_1)$	0.5294	0.5264	0.5246	0.5122
$RITAE_1(C_i,C_1,t_{c1},t_{s1})$	1.5249	1.5005	1.5279	1.2941
$RITAE_2(C_i,C_1,t_{c2},t_{s2})$	0.9586	1.0463	0.9588	0.8236
$RITAE_2(C_i,C_1,t_{c3},t_{s3})$	0.8475	0.7621	0.8670	0.8162
$RITAE_2(C_i,C_1,t_{c4},t_{s4})$	0.2090	0.2034	0.1548	0.2150
$RIAVU_1(C_i,C_1)$	1.0186	1.0193	1.0178	1.0163
$RIAVU_2(C_i,C_1)$	0.8129	0.8363	0.7325	0.8072
$J_c(C_i,C_1)$	**0.7840**	**0.7764**	**0.7749**	**0.7088**

Note: C1=Benchmark PID, C2=SISO-PFMFAC, C3=SISO-PFMFAC-NNSE, C4=SISO-PFMFAC-NNGV, C5=SISO-PFMFAC-NNSEGV
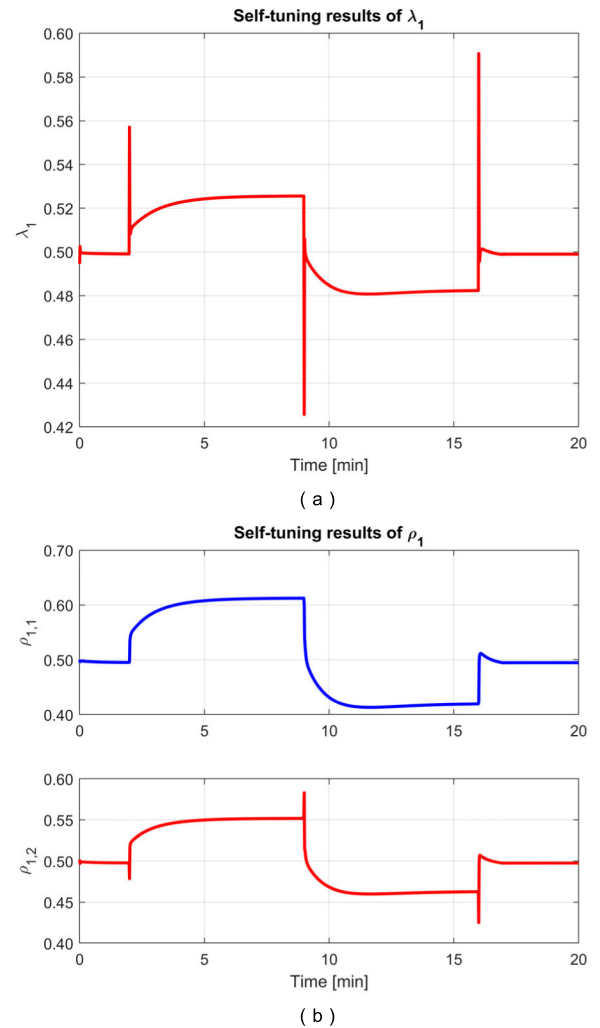

FIGURE 11. Parameter self-tuning results of (a) λ_1 and (b) $\rho_{1,p}$ for expansion valve opening (Av).

and meaningful in the field of control theory. By comparing the last three columns, we can see that SISO-PFMFAC-NNSEGV performs better than SISO-PFMFAC-NNSE and SISO-PFMFAC-NNGV because it contains sufficient information of the system outputs and the dynamics of the control inputs, thus making the parameters self-tune more efficiently.
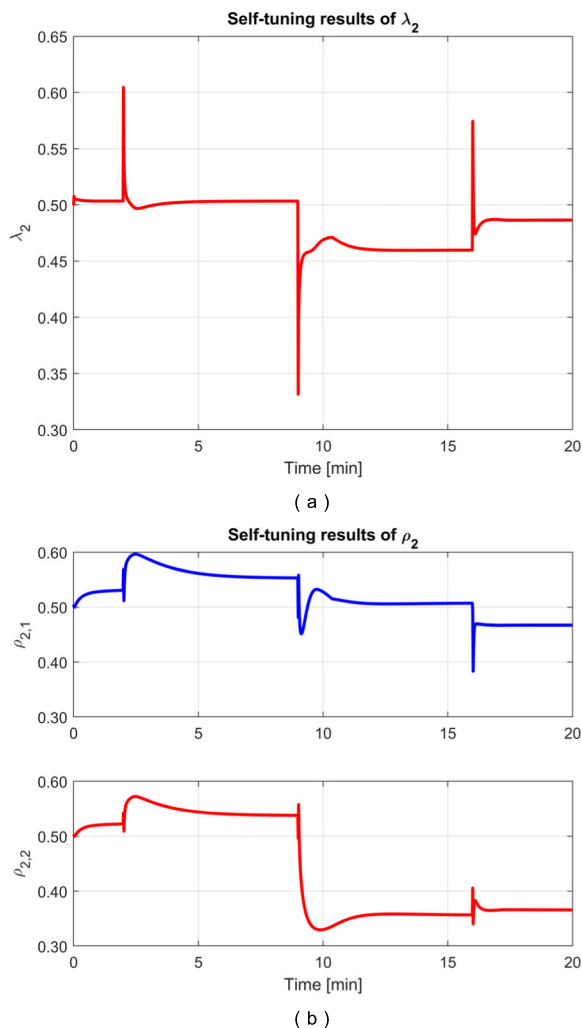
FIGURE 12. Parameter self-tuning results of (a) λ_2 and (b) $\rho_{2,p}$ for compressor speed (N).

focuses on the online self-tuning method using a BP neural network with the system error set and gradient vector set as learning signals, the effectiveness of which has been verified by comparison with the benchmark PID controller. In addition, in order to prove that the dynamic information of the control input is of great significance for the BPNN learning algorithm, a set of comparisons are also given in this work, and the proposed method performs better in both qualitative and quantitative comparisons.

In this work, the performance of the controllers is evaluated though the indices provided in the benchmark, where the combined index J_c plays an important role in the comprehensive performance assessment. The proposed control scheme shows the best performance with $J_c = 0.7088$, which achieves a 29.1% improvement over the benchmark PID controller, a 9.6% improvement over the SISO-PFMFAC controller, an 8.7% improvement over the SISO-PFMFAC-NNSE controller, and an 8.5% improvement over the SISO-PFMFAC-NNGV controller. Furthermore, it shows more accurate trajectories and less variation of the control signals while requiring a simple structure and minimal calculations. More importantly, less variation of the control signals can extend the life of the expansion valve and compressor. Therefore, it can be concluded that the SISO-PFMFAC-NNSEGV controller is an effective method for the parameter self-tuning of SISO-PFMFAC and is also a promising method for the control of vapor-compression refrigeration systems. Our future work will focus on the control of MIMO vapor-compression refrigeration systems.

REFERENCES

[1] G. Bejarano, J. A. Alfaya, M. G. Ortega, and M. Vargas, "On the difficulty of globally optimally controlling refrigeration systems," *Appl. Thermal Eng.*, vol. 111, pp. 1143–1157, Jan. 2017.

[2] L. O. S. Buzelin, S. C. Amico, J. V. C. Vargas, and J. A. R. Parise, "Experimental development of an intelligent refrigeration system," *Int. J. Refrig.*, vol. 28, no. 2, pp. 165–175, Mar. 2005.

[3] X. She, L. Cong, B. Nie, G. Leng, H. Peng, Y. Chen, X. Zhang, T. Wen, H. Yang, and Y. Luo, "Energy-efficient and -economic technologies for air conditioning with vapor compression refrigeration: A comprehensive review," *Appl. Energy*, vol. 232, pp. 157–186, Dec. 2018.

[4] A. Afram, F. Janabi-Sharifi, A. S. Fung, and K. Raahemifar, "Artificial neural network (ANN) based model predictive control (MPC) and optimization of HVAC systems: A state of the art review and case study of a residential HVAC system," *Energy Buildings*, vol. 141, pp. 96–113, Apr. 2017.

[5] K. Jahangeer, A. A. O. Tay, and M. R. Islam, "Numerical investigation of transfer coefficients of an evaporatively-cooled condenser," *Appl. Thermal Eng.*, vol. 31, no. 10, pp. 1655–1663, Jul. 2011.

[6] B. P. Rasmussen, C. Price, J. Koeln, B. Keating, and A. Alleyne, "HVAC system modeling and control: Vapor compression system modeling and control," in *Intelligent Building Control Systems*. Cham, Switzerland: Springer, 2018, pp. 73–103.

[7] A. Goyal, M. A. Staedter, and S. Garimella, "A review of control methodologies for vapor compression and absorption heat pumps," *Int. J. Refrig.*, vol. 97, pp. 1–20, Jan. 2019.

[8] R. Shah, B. P. Rasmussen, and A. G. Alleyne, "Application of a multivariable adaptive control strategy to automotive air conditioning systems," *Int. J. Adapt. Control Signal Process.*, vol. 18, no. 2, pp. 199–221, Mar. 2004.

[9] Y. Shen, W.-J. Cai, and S. Li, "Normalized decoupling control for high-dimensional MIMO processes for application in room temperature control HVAC systems," *Control Eng. Pract.*, vol. 18, no. 6, pp. 652–664, 2010.

Comparing the first column and the last column, almost all indices in the last column are smaller than those of the first column, which indicates that the SISO-PFMFAC-NNSEGV controller has a better tracking performance and less variation of the control signal than SISO-PFMFAC and outperforms in all three parameter self-tuning methods.

In conclusion, from the combined index J_c, the proposed SISO-PFMFAC-NNSEGV controller achieves a 29.1% improvement over the benchmark PID controller, a 9.6% improvement over the SISO-PFMFAC controller, an 8.7% improvement over the SISO-PFMFAC-NNSE controller, and an 8.5% improvement over the SISO-PFMFAC-NNGV controller, making it a promising control method for vapor-compression refrigeration systems.

V. CONCLUSION

In this paper, a self-tuning methodology SISO-PFMFAC-NNSEGV is proposed for the control of vapor-compression refrigeration systems. The proposed controller mainly

[10] L. C. Schurt, C. J. L. Hermes, and A. T. Neto, "A model-driven multivariable controller for vapor compression refrigeration systems," *Int. J. Refrig.*, vol. 32, no. 7, pp. 1672–1682, 2009.

[11] D. Leducq, J. Guilpart, and G. Trystram, "Non-linear predictive control of a vapour compression cycle," *Int. J. Refrig.*, vol. 29, no. 5, pp. 761–772, Aug. 2006.

[12] N. Jain and A. Alleyne, "Exergy-based optimal control of a vapor compression system," *Energy Convers. Manage.*, vol. 92, pp. 353–365, Mar. 2015.

[13] T. G. Hovgaard, L. F. S. Larsen, K. Edlund, and J. B. Jørgensen, "Model predictive control technologies for efficient and flexible power consumption in refrigeration systems," *Energy*, vol. 44, pp. 105–116, Aug. 2012.

[14] A. Afram and F. Janabi-Sharifi, "Theory and applications of HVAC control systems—A review of model predictive control (MPC)," *Building Environ.*, vol. 72, pp. 343–355, Feb. 2014.

[15] T. L. McKinley and A. G. Alleyne, "An advanced nonlinear switched heat exchanger model for vapor compression cycles using the moving-boundary method," *Int. J. Refrig.*, vol. 31, no. 7, pp. 1253–1264, Nov. 2008.

[16] T. K. Nunes, J. V. C. Vargas, J. C. Ordonez, D. Shah, and L. C. S. Martinho, "Modeling, simulation and optimization of a vapor compression refrigeration system dynamic and steady state response," *Appl. Energy*, vol. 158, pp. 540–555, Nov. 2015.

[17] K. J. Astrom and T. Hagglund, *PID Controllers: Theory, Design, and Tuning*, 2nd ed. Triangle Park, NC, USA: Instrument Society of America, 1995.

[18] G. Bejarano, J. A. Alfaya, D. Rodríguez, F. Morilla, and M. G. Ortega, "Benchmark for PID control of refrigeration systems based on vapour compression," *IFAC-PapersOnLine*, vol. 51, no. 4, pp. 497–502, 2018.

[19] Z. Lei and Y. Zhou, "A kind of nonlinear PID controller for Refrigeration Systems based on Vapour Compression," *IFAC-PapersOnLine*, vol. 51, no. 4, pp. 716–721, Jun. 2018.

[20] D. D. Huff, G. R. G. da Silva, and L. Campestrini, "Data-Driven control design by prediction error identification for a refrigeration system based on vapor compression," *IFAC-PapersOnLine*, vol. 51, no. 4, pp. 704–709, Jun. 2018.

[21] Z. Hou and S. Jin, *Model Free Adaptive Control: Theory and Applications*. Boca Raton, FL, USA; CRC press, 2013.

[22] D. Wu, H. Chen, Y. Huang, and S. Chen, "Online monitoring and model-free adaptive control of weld penetration in VPPAW based on extreme learning machine," *IEEE Trans. Ind. Informat.*, vol. 15, no. 5, pp. 2732–2740, May 2019.

[23] Z. Li, Z. Ding, M. Wang, and E. Oko, "Model-free adaptive control for MEA-based post-combustion carbon capture processes," *Fuel*, vol. 224, pp. 637–643, Jul. 2018.

[24] X. Bu, Z. Hou, and H. Zhang, "Data-driven multiagent systems consensus tracking using model free adaptive control," *IEEE Trans. Neural Netw. Learn. Syst.*, vol. 29, no. 5, pp. 1514–1524, May 2018.

[25] H. Zhang, J. Zhou, Q. Sun, J. Guerrero, and D. Ma, "Data-driven control for interlinked AC/DC microgrids via model-free adaptive control and dual-droop control," *IEEE Trans. Smart Grid*, vol. 8, no. 2, pp. 557–571, Mar. 2017.

[26] R. C. Roman, M. B. Radac, R. E. Precup, and E. M. Petriu, "Data-driven model-free adaptive control tuned by virtual reference feedback tuning," *Acta Polytechnica Hungarica*, vol. 13, no. 1, pp. 83–96, Jan. 2016.

[27] L. dos Santos Coelho and A. A. R. Coelho, "Model-free adaptive control optimization using a chaotic particle swarm approach," *Chaos, Solitons Fractals*, vol. 41, no. 4, pp. 2001–2009, Aug. 2009.

[28] K. Cui and X. Qin, "Virtual reality research of the dynamic characteristics of soft soil under metro vibration loads based on BP neural networks," *Neural Comput. Appl.*, vol. 29, no. 5, pp. 1233–1242, Mar. 2018.

[29] L. Bo, L. Huang, Y. Dai, Y. Lu, and K. To Chong, "Mitigation of DC components using adaptive BP-PID control in transformless three-phase grid-connected inverters," *Energies*, vol. 11, no. 8, p. 2047, Aug. 2018.

[30] S. Xing, J. Ju, and J. Xing, "Research on hot-rolling steel products quality control based on BP neural network inverse model," *Neural Comput. Appl.*, vol. 31, no. 5, pp. 1577–1584, May 2019.

CHEN CHEN received the B.S. degree from the College of Automation Engineering, Nanjing University of Aeronautics and Astronautics, Nanjing, China, in 2018. She is currently pursuing the Ph.D. degree with the State Key Laboratory of Industrial Control Technology, College of Control Science and Engineering, Zhejiang University, Zhejiang, China.

Her current research interests include data-driven control, intelligent control, and their industrial applications.
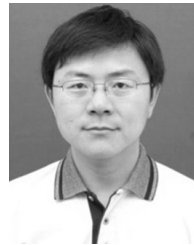
JIANGANG LU received the B.S. and Ph.D. degrees from Zhejiang University, China, in 1989 and 1995, respectively.

He is currently a Full Professor with the Institute of Industrial Process Control and the College of Control Science and Engineering, Zhejiang University. Up to now, he has published one book and more than 120 articles in journals and conferences. His research interests include artificial intelligence in industries, intelligent sense, intelligent modeling, intelligent control, intelligent optimization, and industrial big data. He is a member of the Technical Committee on Process Control, Chinese Association of Automation, and the Standing Director of the Zhejiang Association of Automation. He received the First Prize of China's National Science and Technology Progress Award, in 2013, the Geneva International Invention Gold Medal Award, in 2013, and the Second Prizes of Zhejiang Province Science and Technology Progress Award, in 2007 and in 1999.

• • •